JOC*Article*

Conformation Analyses, Dynamic Behavior, and Amide Bond Distortions of Medium-sized Heterocycles. 2. Partially and Fully Reduced 1-Benzazocines, Benzazonines, and Benzazecines

Maryiam Qadir,[†] Jonathan Cobb,[†] Peter W. Sheldrake,[‡,⊥] Neil Whittall,[‡] Andrew J. P. White,[§] King Kuok (Mimi) Hii,*[,§] Peter N. Horton,[∥] and Michael B. Hursthouse[∥]

Department of Chermistry, King's College London, Strand WC2R 2LS, U.K., GlaxoSmithKline, Old Powder Mills, Tonbridge, Kent, U.K., Department of Chemistry, Imperial College London, Exhibition Road, South Kensington SW7 2AZ, U.K., and EPSRC X-ray Crystallography Service, Southampton University, Highfield SO17 1BJ, U.K.

mimi.hii@imperial.ac.uk

Received October 23, 2004

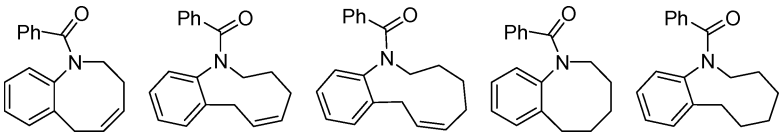

Partially and fully reduced forms of benzo-fused eight- to ten-membered nitrogen heterocycles (1-benzazecines, 1-benzazonines and 1-benzazecines) have been prepared. Conformational features, transannular distances and dynamic behavior were studied using X-ray crystallography and VT NMR spectroscopy. The amide moiety in the nine-membered benzazonine ring **5b** favors *N*-pyramidization, whereas the ten-membered benzazecine **5c** adopts an amide twist. Molecular mechanics calculations reveals a correlation between the amide twist (τ) and ring stability. The dynamic behavior of the heterocycles in solution were also found to be dependent on the extent and nature of the amide distortion. We thus conclude that ring strain of these medium-sized heterocyclic rings is relieved through amide distortion, which leads to a more stable structure.

Introduction

In the preceding paper, we described expedient transition-metal-catalyzed synthetic routes to 1-benzazepine structures. Substitutions introduced at key positions of the heterocyclic ring lead to changes to the solid- and solution-state structures, which were examined using a combination of X-ray crystallography, NMR spectroscopy and molecular mechanics calculations. Part of this study revealed that the reduction of the endocyclic double bond in benzazepine **1** (Figure 1) introduces flexibility to the fully saturated ring **2**, which is able to relieve ring strain by amide distortion. As a result of its greater stability, compound **2** undergoes slower ring inversion than **1**.

Subsequent development of the work led us to extend the study to larger rings. Compared to the 1-benzazepines, corresponding benzo-fused eight-membered heterocyclic rings (1-benzazocines) are relatively uncommon, whereas very few examples of larger nine- and ten-membered analogues (1-benzazonines and 1-benzazecines, respectively) are known beyond the patent literature.[1,2]

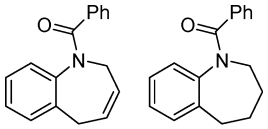

1 **2**

FIGURE 1. Dihydro- and tetrahydro-1-benzazepines.

Results and Discussion

Synthesis of Eight to Ten-Membered Heterocycles (Scheme 1). Following the general procedures described in the preceding article, alkylation of *N*-2-

* To whom correspondence should be addressed. Fax: +44-20-7594-5804. Tel: +44-20-7594-1142.
[†] King's College London.
[‡] GlaxoSmithKline.
[§] Imperial College London.
[∥] Southampton University.
[⊥] Current affiliation: Institute of Cancer Research, 15, Cotswold Rd, Belmont, Sutton, Surrey SM2 5NG, U.K.

(1) (a) Shiraishi, M.; Baba, M.; Aikawa, K.; Kanzaki, N.; Seto, M.; Iizawa, Y. Preparation of 1-benzazocine-5-carboxamides and related bicyclic compounds as CCR-5 antagonists for use against HIV infection and other diseases. World Patent WO2003/014105, 2003. (b) Hamminga, D.; van Wjingaarden, I.; Jansen, J. W. C. M. Preparation of 8,9-annelated-1,2,3,4-tetrahydro-β-carboline derivatives as fibrinolytics. European Patent EP380155, 1990.

(2) Alder, R. W.; White, J. M. In *Conformational Analysis of Medium-Sized Heterocycles*; Glass, R. S., Ed.; VCH: New York, 1988; Chapter 3.

10.1021/jo048117j CCC: $30.25
Published on Web 01/29/2005

SCHEME 1. Synthesis of Heterocycles (Bz = benzoyl; Bn = benzyl)[a]

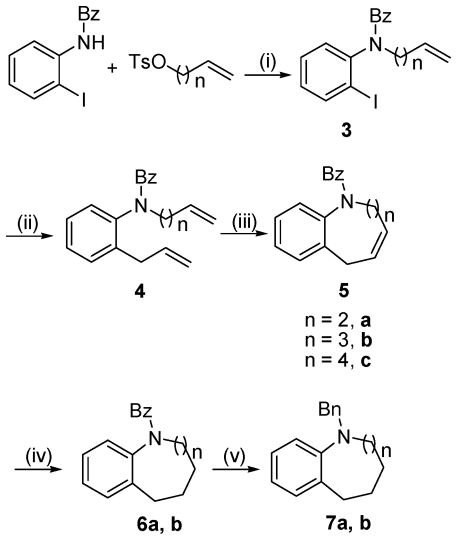

[a] Reagents and conditions: (i) NaH, THF; (ii) (allyl)$SnBu_3$, $Pd(OAc)_2$, PPh_3, LiCl; (iii) Grubb's catalyst, toluene or CH_2Cl_2 (Table 1); (iv) H_2, Pd/C; (v) $BH_3{\cdot}SMe_2$.

TABLE 1. Reaction Conditions Adopted for RCM Reaction[a]

entry	product (ring size)	catalytic loading (mol %)	temp (°C)	solvent	yield[b] *(%)*
1	**5a** (8)	5	60	toluene	81
2	**5b** (9)	5	60	toluene	35
3	**5b** (9)	10	60	toluene	67
4[c]	**5b** (9)	5	35	DCM	78
5	**5c** (10)	5	60	toluene	15
6	**5c** (10)	5	80	toluene	13
7[c]	**5c** (10)	10	60	toluene	17
8[c]	**5c** (10)	10	40	DCM	15

[a] Reaction conducted in 0.1 M solutions in sealed Young's tubes for 22−24 h unless otherwise stated. [b] Isolated yield after column chromatography. [c] Reaction time of 7 days.

iodophenyl-*N*-benzamide with respective 1-alkenyl *p*-toluenesulfonates followed by Stille cross-coupling with allyltributyltin afforded the diene compounds **4a**−**c**.[3] These were subjected to RCM effected by Grubb's catalyst $Ru(=CHPh)Cl_2(PCy_3)_2$ to furnish the novel series of medium-sized heterocycles **5a**−**c**, containing one unit of unsaturation within the ring.

The yield of the RCM reaction is dependent on the ring size being formed, as well as the reaction conditions under which catalysis was effected (Table 1). The eight-membered dehydrobenzazocine ring **5a** was obtained in high yield using previously optimized conditions (entry 1). However, the formation of the larger rings were significantly slower, such that catalyst decomposition became a competitive process under these conditions. Hence, **5b** can only be obtained in moderate to good yields either by adopting higher catalytic loading at 60 °C (entry 3) or a prolonged reaction time at 35 °C (entry 4), whereas the ten-membered benzazecine ring **5c** was only obtained in very small quantities despite our attempts at optimization (entries 5−8). The alkene moiety in all of these heterocycles possesses exclusive *Z*-geometry, as verified by NMR (NOESY) experiments.

The fully saturated forms of the eight- and nine-membered heterocycles **6a**,**b** were then obtained via hydrogenolysis over Pd/C.[4] Reduction of the amide bond is carried out with borane, to give the *N*-benzyl-substituted forms **7a** and **7b** as dense oils.

Fortuitously, *N*-benzoyl compounds **5a**−**c** and **6a**,**b** are sufficiently crystalline to allow analysis of these unusual eight- to ten-membered rings via single-crystal X-ray diffraction. Thus, structural features such as ring conformation, transannular distances and distortion of the exocyclic amide bond may be examined in a systematic manner, as reflected in the amide bond twist and/or *N*-pyramidization through θ, τ, and α values.

Solid-State Structures (Figure 2, Table 2). Both benzazocines **5a** and **6a** display the boat-chair (BC) conformation, with **5a** having an unusually wide internal angle about nitrogen [b = 119.86(11)°]. Overall, transannular interactions in these eight-membered ring structures are negligible; the closest nonbonding distance in **5a** is observed between H-3α and H-6α of approximately 2.39 Å, increasing to 2.59 Å upon reduction of the double bond to **6a**. The nitrogen heteroatom in both structures are relatively planar, the reduced benzazocine **6a** being slightly more distorted than **5a**, presumably due to greater conformational flexibility.

The nine-membered benzazonines **5b** and **6b** adopt boat-chair conformations in the solid state. Unlike the benzazocines, the unsaturated heterocycle **5b** has an amide bond more distorted than that of **6b**, displaying substantial *N*-pyrimidization, due entirely to a χ_N twist of 31.0° (θ = 352.8°, α = 26.0°). This is accompanied by a lengthening of the amide bond [1.373(2) Å]. Notably, there is a very close transannular distance in **5b** between H-4α and H-7α of 2.07 Å. A slight overlap of the van der Waals radii of the two nuclei could be observed in the space-filling model, which could suggest the presence of a small repulsive interaction. When the endocyclic double bond is reduced, the transannular distance between H-4α and H-7α in **6b** becomes greater (2.15 Å). The C−N bond length returns to a more expected value [1.354(2) Å], as the amide moiety becomes essentially planar (θ = 359.7°, α = 5.4°) with negligible twist (τ = 0.4°).

Exhibiting the boat-chair-boat (BCB) conformation, the closest transannular distance in the ten-membered benzoazecine ring **5c** is between H-5α and H-8α (2.10 Å). Interestingly, the nature of the amide distortion is entirely different in this molecule: while the smaller seven- to nine-membered heterocyclic rings distort by *N*-pyramidization (large χ_N), the planarity of the N−C(O) amide bond in the ten-membered ring is retained (θ = 360.0°, α = 0.7°). However, a significant twist between the plane and the N−C′ vector of the amide bond was observed (τ = −16.2°), which implies that the nitrogen lone pair may be able to conjugate with the fused aromatic ring.

Examining the IR spectra of the solid samples (as KBr disks), structures containing the most pyramidized amide bonds (**1**, **2**, and **5b**, where α > 12°) exhibit C=O

(3) The yields of the *N*-alkylation reactions were poor if they were performed after the Stille reaction, presumably due to reduced electrophilicity of these alkenyl tosylates.

(4) Benzoazecine **5c** was not hydrogenated due to the small quantity available.

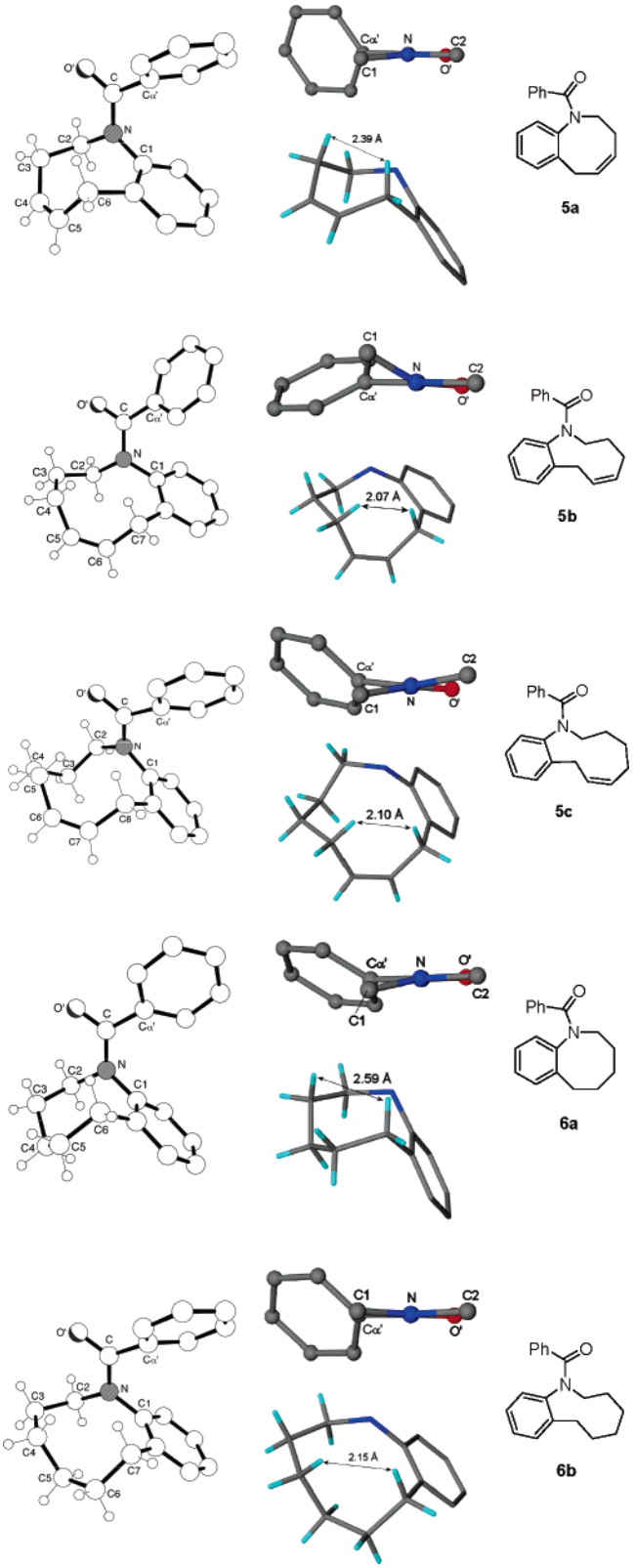

FIGURE 2. Molecular structures of **5a**−**c**, **6a**, and **6b**, with chemical numbering scheme, illustrating transannular distances (middle) and amide distortions (right). Aromatic hydrogens are omitted for clarity.

stretching frequencies approximately 10 cm^{-1} higher than the rest.

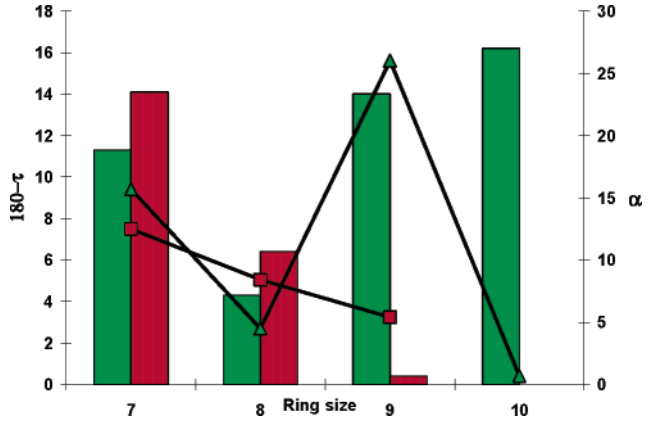

FIGURE 3. Variation of τ and α values with ring size. Columns = 180 − $|\tau|$; data points = $|\alpha|$; green = unsaturated rings; red = saturated rings.

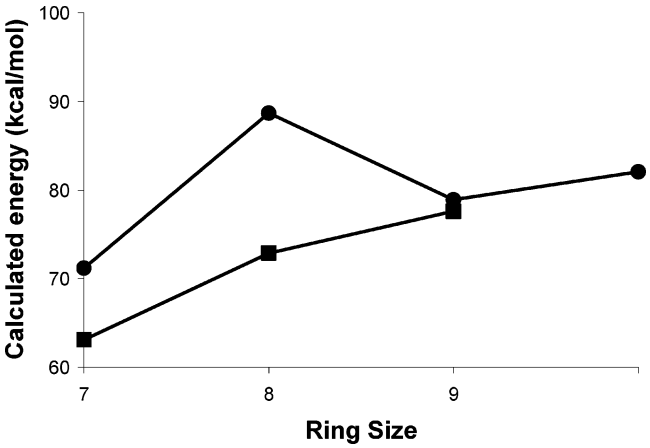

FIGURE 4. Relative energies of seven- to ten-membered rings. Circle = unsaturated rings; squares = saturated rings.

Trends in the Amide Distortions (Figure 3). Previously, we have demonstrated that benzazepine rings are stabilized by amide distortions and the proportional relationship between τ and α. Examining the series of saturated rings (**2**, **6a**, and **6b**), an increase in the ring size appears to lead to a corresponding increase in amide planarity (Figure 3, red columns), accompanied by a smaller amide twist (Figure 3, red squares).

In the unsaturated series (**1**, **5a**, **5b**, and **5c**), the above trend is only observed for the seven- and eight-membered heterocycles (Figure 3, green columns and squares). The nine-membered ring seemed to favor *N*-pyramidization (large α) over amide twist, whereas the opposite is true for the ten-membered ring (large τ).

Molecular Modeling. Assignment of stable conformations of these larger rings by molecular modeling has to be made with great caution. In addition to ring strain, a number of other factors such as entropic freedom and transannular forces are also envisaged to be important, all of which may be affected by crystal packing forces in the solid-state structure. With this in mind, we calculated the energies of the solid-state structures using Spartan mechanics, and the values obtained were plotted against each other to assess the effect of ring expansion (Figure 4). For both the unsaturated and saturated ring systems, there appears to be an overall increase in energy with

TABLE 2. Crystal Structure and Spectroscopic Parameters Reflecting Amide Deformations[a]

compound	b[b]	θ[c]	ω_1[d]	ω_2[e]	ω_3[f]	ω_4[g]	χ_N[h]	χ_C[i]	τ[j]	α[k]	C−N (Å)	ν_{CO}[l] (cm^{-1})
1	115.31(8)	357.3	+182.3	+200.2	+0.8	+21.7	+19.4	+1.5	+191.3 (+11.3)	15.7	1.3662(14)	1644
5a	119.86(11)	359.8	+181.3	+186.8	+1.6	+6.5	+5.2	−0.3	+184.1 (+4.3)	4.5	1.359(2)	1634
5b	115.58(14)	352.8	+179.9	+152.1	+3.1	−31.0	−31.0	−3.2	+166.0 (−14.0)	26.0	1.373(2)	1640
5c	116.84(10)	360.0	+162.8	+166.8	−14.1	−16.3	+0.9	−3.1	+164.8 (−16.2)	0.7	1.366(2)	1630
2	116.67(11)	358.4	+188.1	+200.0	+4.8	+23.3	+15.2	+3.3	+194.1 (+14.1)	12.5	1.368(2)	1640
6a	115.67(11)	359.3	+178.1	+169.1	−0.3	−12.5	−10.6	−1.6	+173.6 (−6.4)	8.4	1.353(2)	1626
6b	117.39(9)	359.7	+182.7	+178.1	+4.7	−3.8	−6.5	−2.0	+180.4 (+0.4)	5.4	1.354(2)	1632

[a] Data for **1** and **2** had been reported in the preceding paper and are reproduced here for comparison. ω_1, ω_2, ω_3, and ω_4 assignments are made as for *trans* amides where C1 = H. Unless otherwise stated, all values are in degrees. [b] Angle C1−N−C2. [c] Sum of angles around N (a + b + c). [d] ω_1 = C$_{\alpha'}$−C′−N−C2 torsion angle. [e] ω_2 = O′−C′−N−C1 torsion angle. [f] ω_3 = O′−C′−N−C2 torsion angle. [g] ω_4 = TORS[C$_{\alpha'}$,C′,N,C1]. [h] $\chi_N = (\omega_2 - \omega_3 + \pi)(\mathrm{mod}\ 2\pi)$ and has a value between 0° (planar) and 60° (complete pyramidization). [i] $\chi_C = (\omega_1 - \omega_3 + \pi)(\mathrm{mod}\ 2\pi)$. [j] $\tau = [(\omega 1 + \omega 2)/2](\mathrm{mod}\ 2\pi)$, where $|\omega_1 - \omega_2| < \pi$ (else τ is mod π). Value in parentheses corresponds to deviation from 180°. [k] α is the angle between the plane and the N−C′ vector. [l] Recorded as KBr disks.

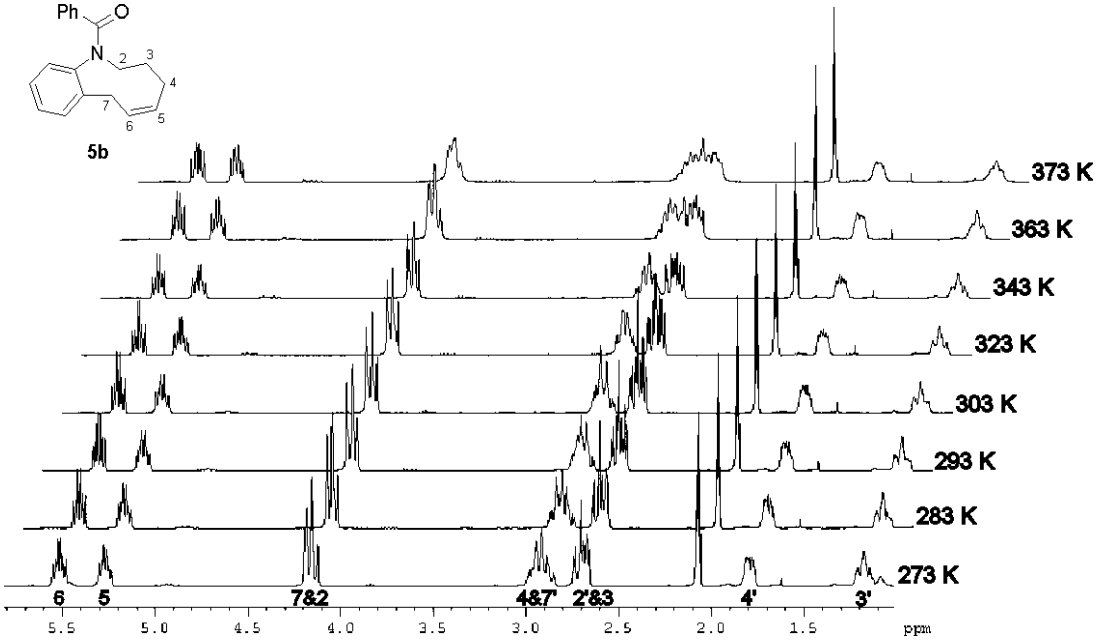

FIGURE 5. Variable temperature ^{1}H NMR spectra of compound **5b** (resonances of heterocyclic ring protons).

ring size. There is a remarkable correlation between the trends of relative energies with the amide twist (Figure 3): an increase in the τ leads to a corresponding rise in stability (lower energy). This reinforced the notion established in our previous study of benzazepine structures, that ring strain of these systems is largely alleviated through amide twist.

Dynamic NMR Behavior. Since greater amide distortion is associated with a more stable ground-state structure, we would also expect a larger activation energy for ring inversion. Although the variable NMR spectra of the larger rings are more complicated, the larger benzazocine rings do indeed appear to have a higher activation barrier to ring flipping than the smaller benzazepine rings. As both benzazocine structures display very little amide distortion, they also have very similar activation energies toward ring inversion, which are estimated to be 16.7 and 17.0 kcal mol^{-1} for **5a** and **6a**, respectively. This is in marked contrast to that observed for benzazepines, where the saturated ring (more distorted amide) is conformationally more stable than the unsaturated ring.

Having more distorted amide bonds, the nine-membered rings also require much higher activation energies to undergo conformational changes. Distinct diastereotopic proton resonances were observed in the NMR spectra of compounds **5b**, **5c**, and **6b**, which undergo very slow exchange on the NMR time scale. As the unsaturated nine-membered benzazonine **5b** has the most distorted amide bond, ring inversion would be expected to be a very unfavorable process. Indeed, the resolution of the resonance signals corresponding to the heterocyclic ring protons is well-preserved over a broad temperature range, showing very little broadening, even at 373 K (Figure 5).

Since the saturated benzazonine **6b** possesses an amide bond less distorted than that of the unsaturated **5b**, we will expect the latter to be conformationally more stable. Qualitative comparison of the VT NMR spectra of **5b** and **6b** indicates that the saturated ring is, indeed, more labile than the unsaturated ring, as indicated by greater broadening of the resonance signals of **6b** at elevated temperatures (Supporting Information).

It is clear from our study that the dynamic behavior of these heterocycles is highly dependent on the nature of the amide bond. Indeed, when the *N*-benzoyl is transformed to an *N*-benzyl moiety, the resultant tetrahydro-benzazocine and benzazonine rings **7a** and **7b**

display extremely fluxional ^{1}H NMR spectra. Signals of individual geminal methylenes could not be resolved, even at the lowest temperature of 183 K (Supporting Information), indicating rapid ring inversion of the fully reduced forms.

In conclusion, a series of seven- to ten-membered benzo-fused nitrogen heterocycles have been prepared. X-ray crystallography revealed that most of the structures contain distorted amides, which may occur through *N*-pyramidization (largely χ_N twist) or by an out-of-plane twist (τ). Molecular modeling revealed a correlation between ring stability and amide twist τ. As a consequence, the dynamic behavior of these rings is dependent on the nature and the extent of the amide distortion. On the whole, greater amide distortion is accompanied by a larger barrier to ring inversion.

Experimental Section

***N*-But-3-en-1-yl-*N*-(2-iodophenyl)benzamide (3a).** Yield: 88% as colorless, rock-like crystals, $R_f = 0.25$, hexanes/EtOAc (5/1); mp 66.2−67.8 °C (from EtOAc/hexanes). Found: C, 54.90; H, 4.10; N, 3.55. Calcd for $C_{17}H_{16}NIO$: C, 55.12; H, 3.91; N, 3.39. ν_{max} (KBr)/cm^{-1} 1634vs br (CO), δ_H (360 MHz; $CDCl_3$) 2.39−2.45 (1H, br m, C*H*HCH$_2$N), 2.48−2.54 (1H, br m, CH*H*CH$_2$N), 3.37−3.45 (1H, br m, C*H*HN), 4.40−4.48 (1H, br m, CH*H*N), 5.08−5.16 (2H, br m, C*H*$_2$=CHCH$_2$), 5.80−5.92 (1H, br m, CH$_2$=C*H*CH$_2$), 6.89−6.94 (1H, br m, Ar-H), 7.08 (1H, d, *J* 7.4, Ar-H), 7.13−7.23 (4H, m, Ar-H), 7.35 (2H, br d, *J* 7.3, Ar-H), 7.82 (1H, d, *J* 7.8, Ar-H); δ_C (100.6 MHz; $CDCl_3$) 32.1 (1C, *C*H$_2$CH$_2$N), 49.1 (1C, CH$_2$N), 100.5 (1C, C$_2$), 117.2 (1C, *C*H$_2$=CHCH$_2$), 128.0, 128.6, 129.3, 129.5, 130.0 (Ar-C), 132.2 (1C, C$_6$), 135.7 (1C, CH$_2$=*C*HCH$_2$), 136.5, 140.6, 145.4 (Ar-C), 170.8 (1C, CO); *m/z* (EI) 377 (M$^+$, 4%), 336 (22), 323 (12), 250 (47), 208 (3), 196 (6), 105 (100), 77 (27).

***N*-Hex-5-en-1-yl-*N*-(2-iodophenyl)benzamide (3c).** Yield: 80% as a pale yellow syrup which crystallized upon standing, $R_f = 0.23$, hexanes/EtOAc (4/1); mp 65.0−66.6 °C (from EtOAc/hexanes). Found: C, 56.20; H, 4.75; N, 3.30. Calcd for $C_{19}H_{20}NIO$: C, 56.30; H, 4.98; N, 3.46. ν_{max} (KBr)/cm^{-1} 1623br vs (CO); δ_H (360 MHz; $CDCl_3$) 1.27 (br s, rotamer), 1.41−1.63 (3H, br m, C*H*HCH$_2$N, C*H*$_2$CH$_2$CH$_2$N,), 1.76−1.85 (1H, br m, CH*H*CH$_2$N), 1.91 (br s, rotamer), 2.08−2.13 (2H, br m, CH$_2$=CHC*H*$_2$), 3.32−3.40 (1H, br m, C*H*HN), 3.65 (br s, rotamer), 4.33 (1H, ddd, *J* 3.5, 5.7 and 10.1, CH*H*N), 4.94−5.03 (2H, br m, C*H*$_2$=CHCH$_2$), 5.75−5.86 (1H, m, CH$_2$=C*H*CH$_2$), 6.89−6.93 (1H, m, Ar-H), 7.05 (1H, d, *J* 7.1, Ar-H), 7.13−7.24 (4H, m, Ar-H), 7.35 (2H, d, *J* 7.2, Ar-H), 7.48−7.67 (br s, rotamer), 7.82 (1H, d, *J* 7.9, Ar-H), 7.97 (br s, rotamer); δ_C (100.6 MHz; $CDCl_3$) 26.8 (1C, *C*H$_2$CH$_2$N), 27.1 (1C, *C*H$_2$-CH$_2$CH$_2$N), 33.9 (1C, CH$_2$=CH*C*H$_2$), 49.8 (1C, CH$_2$N), 100.5 (1C, C$_2$), 115.1 (1C, *C*H$_2$=CHCH$_2$), 128.0, 128.6 (4C, C$_{ortho}$, C$_{meta}$), 129.3, 129.4, 130.5, 132.0, 136.3 (Ar-C), 138.9 (1C, CH$_2$=*C*HCH$_2$), 140.7, 145.6 (Ar-C), 170.7 (1C, CO); *m/z* (EI) 405 (M$^+$, 4%), 323 (13), 278 (100), 196 (20), 105 (78), 77 (28).

***N*-(2-Allylphenyl)-*N*-(but-3-en-1-yl)-benzamide (4a).** Yield: 68% as a colorless syrup, $R_f = 0.22$, hexanes/EtOAc (5/1). Found: C, 82.55; H, 7.50; N, 4.90. Calcd for $C_{20}H_{21}NO$: C, 82.42; H, 7.28; N, 4.81. ν_{max} (thins film)/cm^{-1} 1644vs br (CO); δ_H (360 MHz; $CDCl_3$) 2.32−2.42 (2H, br m, C*H*$_2$CH$_2$N), 3.11 (1H, dd, *J* 6.3 and 9.4, ArC*H*H), 3.28 (1H, dd, *J* 6.8 and 9.4, ArCH*H*), 3.44 (1H, ddd, *J* 4.3, 6.3 and 9.0, C*H*HN), 4.18 (1H, ddd, *J* 4.1, 6.3 and 9.0, CH*H*N), 4.97−5.06 (4H, br m, ArCH$_2$-CH=C*H*$_2$, C*H*$_2$=CHCH$_2$), 5.61−5.79 (2H, br m, ArCH$_2$C*H*=CH$_2$, CH$_2$=C*H*CH$_2$), 6.99−7.48 (9H, m, ArH); δ_C (90.6 MHz; $CDCl_3$) 32.1 (*C*H$_2$CH$_2$N), 35.3 (ArCH$_2$), 49.9 (CH$_2$N), 117.1 (*C*H$_2$=CHCH$_2$), 117.5 (ArCH$_2$CH=*C*H$_2$), 127.4, 127.9, 128.2, 128.7, 129.9, 130.3, 130.9 (Ar-C), 135.7 (CH$_2$=*C*HCH$_2$), 136.2 (ArCH$_2$*C*H=CH$_2$), 136.5, 137.4, 141.8 (Ar-C), 170.8 (CO); *m/z* (EI) 291 (M$^+$, 12%), 250 (46), 236 (6), 186 (5), 105 (100), 77 (25).

***N*-(2-Allylphenyl)-*N*-(pent-4-en-1-yl)-benzamide (4b).** Yield: 84% as a pale yellow syrup, $R_f = 0.23$, hexanes/EtOAc (5/1). Found: C, 82.80; H, 7.75; N, 4.75. Calcd for $C_{21}H_{23}NO$: C, 82.57; H, 7.61; N, 4.59. ν_{max} (neat)/cm^{-1} 1644br s (CO); δ_H (400 MHz; $CDCl_3$) 1.62−1.76 (2H, br m, C*H*$_2$CH$_2$N), 1.98−2.09 (2H, C*H*$_2$CH$_2$CH$_2$N), 3.10 (1H, dd, *J* 6.3 and 9.4, ArC*H*H), 3.27 (1H, dd, *J* 6.8 and 9.4, ArCH*H*), 3.42 (1H, ddd, *J* 2.7, 5.2 and 10.5, C*H*HN), 4.05 (1H, ddd, *J* 2.7, 5.7 and 10.5, CH*H*N), 4.87−5.03 (4H, m, ArCH$_2$CH=C*H*$_2$, C*H*$_2$=CHCH$_2$), 5.58−5.76 (2H, m, ArCH$_2$C*H*=CH$_2$, CH$_2$=C*H*CH$_2$), 5.77 (br s, rotamer), 6.98−7.19 (9H, ArH), 7.21−7.38 (br m, rotamer); δ_C (100.6 MHz; $CDCl_3$) 26.8 (*C*H$_2$CH$_2$N), 31.7 (*C*H$_2$CH$_2$CH$_2$N), 35.3 (ArCH$_2$), 50.4 (CH$_2$N), 115.4 (*C*H$_2$=CHCH$_2$), 117.5 (ArCH$_2$CH=*C*H$_2$), 127.4, 127.9, 128.8, 130.1, 130.9 (ArC), 136.2 (ArCH$_2$*C*H=CH$_2$), 136.5, 137.4 (Ar-C), 138.2 (CH$_2$=*C*HCH$_2$), 141.9 (Ar-C), 170.7 (1C, CO); *m/z* (EI) 305 (M$^+$, 66%), 262 (100), 236 (30), 200 (68), 105 (99), 77 (79).

***N*-(2-Allylphenyl)-*N*-(hex-5-en-1-yl)-benzamide (4c).** Yield: 87% as a pale yellow syrup, $R_f = 0.27$, hexanes/EtOAc (5/1). Found: C, 82.85; H, 8.10; N, 4.55. Calcd for $C_{22}H_{25}NO$: C, 82.70; H, 7.90; N, 4.39. ν_{max} (thin film)/cm^{-1} 1643 br vs (CO); δ_H (400 MHz; $CDCl_3$) 1.19 (br s, rotamer), 1.32−1.41 (2H, br m, C*H*$_2$CH$_2$CH$_2$N), 1.50−1.69 (2H, br m, C*H*$_2$CH$_2$N), 1.85 (br s, rotamer), 1.97−2.03 (2H, m, CH$_2$=CHC*H*$_2$), 3.18 (1H, dd, *J* 6.3 and 9.3, ArC*H*H), 3.27 (1H, dd, *J* 6.8 and 9.3, ArCH*H*), 3.41 (1H, ddd, *J* 2.8, 5.4 and 10.3, C*H*HN), 4.05 (1H, ddd, *J* 2.9, 5.8 and 10.3, CH*H*N), 4.84−5.03 (4H, br m, ArCH$_2$CH=C*H*$_2$, C*H*$_2$=CHCH$_2$), 5.58−5.76 (2H, br m, ArCH$_2$C*H*=CH$_2$, CH$_2$=C*H*CH$_2$), 6.98−7.19 (9H, m, ArH), 7.25 (rotamer); δ_C (100.6 MHz; $CDCl_3$) 26.8 (*C*H$_2$CH$_2$CH$_2$N), 27.2 (*C*H$_2$CH$_2$N), 33.9 (CH$_2$=CH*C*H$_2$), 35.3 (ArCH$_2$), 50.7 (1C, CH$_2$N), 115.1 (*C*H$_2$=CHCH$_2$), 117.5 (ArCH$_2$CH=*C*H$_2$), 127.4, 127.9, 128.1, 128.7, 129.9, 130.1, 130.9 (Ar-C), 136.2 (ArCH$_2$*C*H=CH$_2$), 136.6, 137.4 (Ar-C), 138.9 (CH$_2$=*C*HCH$_2$), 141.9 (Ar-C), 170.7 (CO); *m/z* (EI) 319 (M$^+$, 30%), 250 (10), 236 (14), 196 (9), 105 (100), 77 (30).

(4*Z*)-1-Benzoyl-1,2,3,6-tetrahydro-1-benzazocine (5a). Colorless crystals, $R_f = 0.27$, hexanes/EtOAc (3/1); mp 83.9−84.3 °C (from EtOAc/hexanes). Found: C, 82.20; H, 6.65; N, 5.40. Calcd for $C_{18}H_{17}NO$: C, 82.09; H, 6.52; N, 5.32. ν_{max} (KBr)/cm^{-1} 1634vs (CO); δ_H (400 MHz; $CDCl_3$) 2.33−2.40 (1H, m, *H*-3β), 2.67−2.75 (1H, m, *H*-3α), 2.79−2.85 (1H, m, *H*-2β), 3.16 (1H, dd, *J* 6.9 and 14.3, *H*-6β), 3.65 (1H, dd, *J* 7.3 and 14.3, *H*-6α), 4.95 (1H, ddd, *J* 2.2, 7.5 and 13.1, H-2α), 5.76−5.83 (1H, m, *H*-4), 5.90−6.98 (1H, m, *H*-5), 7.08−7.10 (1H, m, ArH), 7.14−7.56 (8H, m, ArH); δ_C (100.6 MHz; $CDCl_3$) 26.9 (*C*-3), 33.6 (*C*-6), 49.0 (*C*-2), 127.7, 128.0, 128.2, 128.5 (Ar-C), 129.2 (*C*-4), 129.6, 130.1, 130.2 (Ar-C), 131.2 (*C*-5), 137.0, 140.7, 142.4 (Ar-C), 170.5 (CO); *m/z* (EI) 263 (M$^+$, 85%), 158 (27), 130 (5), 105 (100), 77 (40). **Crystal data for 5a** (CCDC 251229): $C_{18}H_{17}NO$, MW = 263.33, monoclinic, $P2_1/c$ (No. 14), a = 8.20040(10), b = 22.6060(5), c = 8.51990(10) Å, β = 117.5990(10)°, V = 1399.69(4) Å^3, $Z = 4$, D_c = 1.250 g cm^{-3}, μ(Mo Kα) = 0.077 mm^{-1}, T = 120 K, colorless plates; 3171 independent measured reflections, F^2 refinement, $R_1 = 0.050$, $wR_2 = 0.126$, 2772 independent observed absorption-corrected reflections [$|F_o| > 4\sigma(|F_o|)$, $2\theta_{max} = 55°$], 182 parameters.

(5*Z*)-1-Benzoyl-2,3,4,7-tetrahydro-1H-1-benzazonine (5b). Colorless crystals, $R_f = 0.31$, hexanes/EtOAc (3/1); mp 122.6−124 °C (from EtOH/Et$_2$O). Found: C, 82.35; H, 7.05; N, 5.15. Calcd for $C_{19}H_{19}NO$: C, 82.26; H, 6.92; N, 5.05. ν_{max} (KBr)/cm^{-1} 1640vs (CO); δ_H (400 MHz; $CDCl_3$) 1.41−1.50 (1H, m, *H*-3β), 2.04−2.11 (1H, m, *H*-4β), 2.80−2.86 (1H, m, *H*-3α), 2.92−3.05 (3H, m, *H*-7β, *H*-2β and *H*-4α), 4.17 (1H, ddd, *J* 2.0, 4.2 and 13.2, *H*-2α), 4.23−4.29 (1H, m, *H*-7α), 5.52 (1H, td, *J* 6.0 and 10.7, *H*-5), 5.72 (1H, td, *J* 6.0 and 10.7, *H*-6), 6.73 (1H, dd, *J* 1.3 and 7.8, ArH), 6.93−6.98 (1H, m, ArH), 7.08−7.26 (5H, m, ArH), 7.35−7.38 (2H, m, ArH); δ_C (100.6 MHz; $CDCl_3$) 22.9 (*C*-4), 26.4 (*C*-3), 31.8 (*C*-7), 51.9 (*C*-2), 127.9, 128.2, 128.4, 124.0 (Ar-C), 129.0 (*C*-5), 129.4 (*C*-6), 130.1, 130.2, 131.4 (Ar-C), 136.8, 137.6, 145.8 (Ar-C), 172.8 (CO); *m/z* (EI) 277 (M$^+$, 42%), 249 (22), 222 (6), 172 (71), 130 (21), 105 (100), 91 (8), 77

(58). **Crystal data for 5b** (CCDC 251230): $C_{19}H_{19}NO$, MW = 277.35, monoclinic, $P2_1/c$ (No. 14), a = 9.5717(4), b = 8.2880(3), c = 18.8257(8) Å, β = 92.399(2)°, V = 1492.14(10) Å^3, Z = 4, D_c = 1.235 g cm^{-3}, μ(Mo Kα) = 0.076 mm^{-1}, T = 120 K, colorless shards; 3402 independent measured reflections, F^2 refinement, R_1 = 0.049, wR_2 = 0.100, 1946 independent observed absorption-corrected reflections [$|F_o| > 4\sigma(|F_o|)$, $2\theta_{max} = 55°$], 191 parameters.

(6*Z*)-1-Benzoyl-1,2,3,4,5,8-hexahydro-1-benzazecine (5c). Unreacted diene was recovered in 30% yield while TLC analysis indicated significant amounts of polymerized side products. Colorless crystals, R_f = 0.34, hexanes/EtOAc (3/1); mp 134.6−135.7 °C (from EtOAc/hexanes). Found: C, 82.25; H, 7.00; N, 4.70. Calcd for $C_{20}H_{21}NO$: C, 82.42; H, 7.28; N, 4.81. ν_{max} (KBr)/cm^{-1} 1630vs (CO); δ_H (400 MHz; $CDCl_3$) 1.24−1.31 (2H, m, *H*-3), 1.40−1.47 (1H, m, *H*-4β), 1.83−1.90 (1H, m, *H*-4α), 1.95−1.99 (1H, m, *H*-5β), 2.21 (1H, dd, *J* 6.0 and 13.0, *H*-8β), 2.61−2.71 (1H, m, *H*-5α), 3.36 (1H, dd, *J* 11.0 and 13.0, *H*-8α), 3.55 (1H, dt, *J* 3.5 and 13.4, *H*-2α), 4.81−4.87 (1H, m, *H*-2β), 5.17 (1H, td, *J* 4.8 and 11.0, *H*-6), 5.45 (1H, td, *J* 6.1 and 11.0, *H*-7), 6.91 (1H, dd, *J* 1.3 and 7.7, ArH), 7.00−7.17 (4H, m, ArH), 7.18−7.20 (3H, m, ArH), 7.31 (1H, dd, *J* 1.0 and 7.9, ArH); δ_C (100.6 MHz; $CDCl_3$) 20.9 (*C*-3), 22.7 (*C*-5), 28.9 (*C*-4), 30.1 (*C*-8), 51.1 (*C*-2), 127.5, 127.7, 127.9, 128.2 (ArC), 129.1 (*C*-7), 129.1, 129.8 (ArC), 130.5 (*C*-6), 131.3, 137.1, 139.6, 140.6 (Ar-C), 170.5 (CO); *m/z* (EI) 291 (M$^+$, 34%), 263 (34), 237 (8), 209 (6), 186 (76), 144 (5), 130 (11), 105 (100), 77 (38). **Crystal data for 5c** (CCDC 251231): $C_{20}H_{21}NO$, MW = 291.38, monoclinic, $C2/c$ (No. 15), a = 11.1017(3), b = 11.9013(4), c = 24.0165(7) Å, β = 101.880(2)°, V = 3105.21(16) Å^3, Z = 4, D_c = 1.247 g cm^{-3}, μ(Mo Kα) = 0.076 mm^{-1}, T = 120 K, light brown blocks; 3459 independent measured reflections, F^2 refinement, R_1 = 0.041, wR_2 = 0.092, 2687 independent observed absorption-corrected reflections [$|F_o| > 4\sigma(|F_o|)$, $2\theta_{max} = 55°$], 200 parameters.

1-Benzoyl-1,2,3,4,5,6-hexahydro-1-benzazocine (6a). Yield: 93% as colorless crystals, R_f = 0.21, hexanes/EtOAc (3/1); mp 95.1−95.5 °C (from EtOAc/hexanes). Found: C, 81.25; H, 7.05; N, 5.05. Calcd for $C_{18}H_{19}NO$: C, 81.46; H, 7.23; N, 5.28. ν_{max} (KBr)/cm^{-1} 1626vs (CO); δ_H (400 MHz; $CDCl_3$) 1.28−1.45 (3H, br m, *H*-5α, *H*-4 and *H*-3α), 1.53−1.59 (1H, br m, *H*-4), 1.72−1.78 (1H, br m, *H*-3β), 1.80−1.87 (1H, m, *H*-5β), 2.43 (1H, dt, *J* 4.0 and 13.0, *H*-6β), 2.69 (1H, td, *J* 3.8 and 13.0, *H*-6α), 2.94 (1H, ddd, *J* 3.0, 7.5 and 13.3, *H*-2β), 4.81−4.87 (1H, m, *H*-2α), 6.98−7.15 (7H, m, ArH), 7.19−7.48 (2H, m, ArH); δ_C (100.6 MHz; $CDCl_3$) 26.4, 26.5 (*C*-4 and *C*-3), 31.3, 31.6 (*C*-6 and *C*-5), 51.8 (*C*-2), 127.5, 127.7, 128.2, 128.7, 129.0, 129.4, 130.2, 136.8, 141.5, 142.0 (Ar-C), 170.9 (CO); *m/z* (EI) 265 (M$^+$, 98%), 160 (70), 144 (65), 129 (25), 118 (22), 105 (100), 77 (74). **Crystal data for 6a** (CCDC 251232): $C_{18}H_{19}NO$, MW = 265.34, orthorhombic, $Pna2_1$ (No. 33), a = 10.5641(3), b = 15.7433(5), c = 8.3622(2) Å, V = 1390.75(7) Å^3, Z = 8, D_c = 1.267 g cm^{-3}, μ(Mo Kα) = 0.078 mm^{-1}, T = 120 K, colorless blocks; 3148 independent measured reflections, F^2 refinement, R_1 = 0.035, wR_2 = 0.077, 2747 independent observed absorption-corrected reflections [$|F_o| > 4\sigma(|F_o|)$, $2\theta_{max} = 55°$], 182 parameters. The absolute structure of **6a** could not be reliably determined [$x^+ = +0.1(13)$].

1-Benzoyl-2,3,4,5,6,7-hexahydro-1H-1-benzazonine (6b). Yield: 91% as colorless prisms, R_f = 0.33, hexanes/EtOAc (3/1); mp 102.5−103.8 °C (from EtOAc/hexanes). Found: C, 81.90; H, 7.75; N, 5.10. Calcd for $C_{19}H_{21}NO$: C, 81.67; H, 7.60; N, 5.01. ν_{max} (KBr)/cm^{-1} 1632vs (CO); δ_H (400 MHz; $CDCl_3$) 0.88−0.93 (1H, br m, $ArCH_2CH_2CH$-5α), 1.38−1.61 (4H, br m, *H*-6, *H*-5β and 2 × *H*-4), 1.62−1.74 (2H, br m, *H*-6, *H*-3β), 2.11−2.20 (1H, br m, *H*-3α), 2.25 (1H, dt, *J* 4.4 and 14.0, H-7β), 2.73 (1H, ddd, *J* 4.1, 11.7 and 14.0, *H*-7α), 3.10−3.17 (1H, m, *H*-2β), 4.65 (1H, ddd, *J* 4.3, 5.9 and 13.7, *H*-2α), 6.94 (1H, d, *J* 7.2, ArH), 7.02−7.21 (8H, ArH); δ_C (90.6 MHz; $CDCl_3$) 22.5 (*C*-5), 24.2 (*C*-4), 26.7 (*C*-3), 29.2 (*C*-6), 30.4 (*C*-7), 50.8 (*C*-2), 127.6, 127.7, 128.4, 128.5, 128.8, 129.5, 131.0, 137.1, 140.5, 144.2 (Ar-C), 170.6 (CO); *m/z* (EI) 279 (M$^+$, 79%), 236 (5), 211 (20), 174 (42), 134 (8), 118 (14), 105 (100), 77 (41). **Crystal data for 6b** (CCDC 251233): $C_{19}H_{21}NO$, MW = 279.37, monoclinic, $P2_1/c$ (No. 14), a = 11.3938(4), b = 14.0951(6), c = 9.4791(4) Å, β = 92.901(2)°, V = 1520.36(11) Å^3, Z = 4, D_c = 1.221 g cm^{-3}, μ(Mo Kα) = 0.075 mm^{-1}, T = 120 K, colorless blocks; 3442 independent measured reflections, F^2 refinement, R_1 = 0.043, wR_2 = 0.098, 2526 independent observed absorption-corrected reflections [$|F_o| > 4\sigma(|F_o|)$, $2\theta_{max} = 55°$], 191 parameters.

1-Benzyl-1,2,3,4,5,6-hexahydro-1-benzazocine (7a). Yield: 89% as a colorless oil, R_f = 0.86, hexanes/EtOAc (3/1). Found: C, 86.25; H, 8.55; N, 5.45. Calcd for $C_{18}H_{21}N$: C, 86.00; H, 8.44; N, 5.57. δ_H (360 MHz; $CDCl_3$) 1.09−1.16 (2H, br m, *H*-3), 1.45−1.54 (2H, m, *H*-4), 1.59−1.65 (2H, m, *H*-5), 2.64 (2H, t, *J* 5.9, *H*-2), 2.86 (2H, t, *J* 5.8, *H*-6), 4.08 (2H, s, $PhCH_2$), 7.00−7.03 (1H, m, ArH), 7.09 (1H, dd, *J* 1.2 and 7.4, ArH), 7.14−7.19 (3H, m, ArH), 7.22−7.26 (2H, m, ArH), 7.40 (2H, d, *J* 7.4, ArH); δ_C (100.6 MHz; $CDCl_3$) 27.2 (*C*-3), 28.5 (*C*-4), 33.2 (*C*-6 and *C*-5), 59.3 (*C*-2), 61.3 ($PhCH_2$), 123.1, 125.5, 127.2, 127.4, 128.6, 129.1, 129.9, 140.6, 143.2, 150.9 (Ar-C); *m/z* (EI) 251 (M$^+$, 100%), 160 (95), 132 (16), 118 (21), 91 (56).

1-Benzyl-2,3,4,5,6,7,-hexahydro-1H-1-benzazonine (7b). Yield: 91% as a colorless oil, R_f = 0.67, hexanes/EtOAc (3/1). Found: C, 86.15; H, 8.60; N, 5.05. Calcd for $C_{19}H_{23}N$: C, 85.97; H, 8.75; N, 5.28. δ_H (400 MHz; Tol-d_8; 373 K) 0.98−1.04 (2H, m, *H*-3), 1.26−1.32 (2H, m, *H*-4), 1.39−1.43 (2H, m, *H*-5), 1.50−1.55 (2H, m, *H*-6), 2.63−2.66 (2H, m, *H*-7), 2.72 (2H, t, *J* 5.6, *H*-2), 3.76 (2H, s, $PhCH_2$), 6.80−6.97 (7H, m, ArH), 7.07−7.09 (2H, m, ArH); δ_C (100.6 MHz; $CDCl_3$) 25.5 (*C*-3), 26.9, 27.1 (*C*-6 and *C*-4), 29.6 (*C*-5), 32.9 (*C*-7), 57.1 (*C*-2), 62.6 ($PhCH_2$), 124.6, 126.0, 127.2, 127.3, 128.4, 129.9, 136.6, 140.0, 143.9, 151.6 (Ar-C); *m/z* (EI) 265 (M$^+$, 46%), 222 (6), 208 (16), 174 (89), 145 (14), 118 (36), 91 (100).

Acknowledgment. The synthetic work was conducted at the Department of Chemistry, King's College London by M.Q., supported by an EPSRC industrial CASE award by GlaxoSmithKline (number: 00314292). We thank Johnson Matthey plc for the generous loan of palladium salts.

Supporting Information Available: Crystallographic data for compounds **5a**, **5b**, **5c**, **6a**, and **6b** and selected NMR spectra. This material is available free of charge via the Internet at http://pubs.acs.org.

JO048117J